

NACA RM L55L28

7671

NACA

Fig # 10057

TECH LIBRARY KAFB, NM

0144173



RESEARCH MEMORANDUM

EXPERIMENTAL RESULTS FROM A TEST IN ROUGH AIR AT HIGH
 SUBSONIC SPEEDS OF A TAILLESS ROCKET MODEL HAVING
 CRUCIFORM TRIANGULAR WINGS, AND A NOTE ON THE
 CALCULATION OF MEAN SQUARE LOADS OF
 AIRCRAFT IN CONTINUOUS ROUGH AIR

By A. James Vitale and Jesse L. Mitchell

Langley Aeronautical Laboratory
Langley Field, Va.

HADC
TECHNICAL LIBRARY
AEL 2811

**NATIONAL ADVISORY COMMITTEE
 FOR AERONAUTICS**

WASHINGTON

April 13, 1956

Classification code has (or changed to) Unclassified

By Authority of Nav Tech Pk Announcement #123
(OFFICER) (GRADE CHANGE)

By NAME (S) J. Jensen

.....
(GRADE OF OFFICER MAKING CHANGE) AK

27 March 61
DATE



NATIONAL ADVISORY COMMITTEE FOR AERONAUTICS

RESEARCH MEMORANDUM

EXPERIMENTAL RESULTS FROM A TEST IN ROUGH AIR AT HIGH
SUBSONIC SPEEDS OF A TAILLESS ROCKET MODEL HAVING
CRUCIFORM TRIANGULAR WINGS, AND A NOTE ON THE
CALCULATION OF MEAN SQUARE LOADS OF
AIRCRAFT IN CONTINUOUS ROUGH AIR

By A. James Vitale and Jesse L. Mitchell

SUMMARY

Results from a flight test in continuous rough air at transonic speeds are presented for a rocket model having cruciform, 60° triangular wings. The variation of root-mean-square acceleration increment with Mach number showed a large increase between Mach numbers of 0.82 and 0.88 that is probably associated with a decrease in damping in pitch for the configuration.

The cruciform-wing arrangement for rocket-propelled model rough-air tests was evaluated and appears to be useful for improving the accuracy of the results. An extension of the cruciform arrangement to different wings on one model is also discussed.

A simplified chart, based on power spectral methods of generalized harmonic analysis, is presented for making rapid estimations of the mean square acceleration of aircraft, especially for configurations with low damping, for flight through continuous rough air.

INTRODUCTION

The need for experimental data at transonic and supersonic speeds on the response of airplanes and missiles to gusts and associated gust loads led to the development of a program which utilizes rocket-powered models for rough-air tests. The testing technique, which is still in the development stage, has been used primarily to investigate the effects of changes in configuration and dynamic longitudinal stability on gust

loads at transonic speeds. The characteristics of loads in rough air from several rocket model tests are presented in references 1 and 2 for three configurations having high aspect ratio 45° sweptback wings. The results of these tests indicated the large influence of airplane damping in pitch on gust loads and also indicated that the testing technique used was primarily suitable for investigating large-order effects because of the lack of precision of the test results.

As a continuation of the program investigating the effects of changes in configuration on gust loads a rough-air test was made on a tailless configuration having a highly swept, low aspect ratio wing. The wing chosen was a 60° triangular wing, as a recent wind-tunnel test (ref. 3) indicated a sharp reduction in damping in pitch for a tailless, 60° triangular wing airplane model in the transonic region.

As an additional part of this investigation a cruciform-wing arrangement was used in an attempt to evaluate some of the problems of accuracy which have been found to be inherent with rocket-propelled model tests in rough air.

The Mach number range covered in the test was about 0.66 to 0.92. The test results for this model are evaluated in order to establish the loads and their variation with Mach number. In addition, the use of a cruciform-wing arrangement is discussed in connection with possible improvement of accuracy of results and as an extension of the testing technique.

A method and chart for obtaining calculated values of mean square acceleration for flight through continuous rough air are presented in the appendix of this report. Calculated values from the chart are compared with the experimental values of root-mean-square acceleration from the 60° triangular wing model.

SYMBOLS

a_n	normal acceleration increment, g units
a_t	transverse acceleration increment, g units
a	damping-in-pitch factor, $-\frac{0.693}{T_{1/2}}$, 1/sec
\bar{c}	mean aerodynamic chord, ft
I_y	moment of inertia about transverse axis, slug-ft ²

I_z	moment of inertia about vertical axis, slug-ft ²
k_y	radius of gyration about transverse axis, ft
K_a	constant in equation of turbulence spectrum
L	scale of turbulence, ft
m	mass, slugs
M	Mach number
q	dynamic pressure, lb/ft ²
S	wing area, ft ²
$\hat{T}(i\Omega)$	airplane normal acceleration frequency response function for a sinusoidal gust-velocity input
t	time, sec
t_p	time for the acceleration due to a sharp-edge gust to reach a maximum value, sec
$T_{1/2}$	time to damp to one-half amplitude, sec
$(a_n)_{max}$	peak normal acceleration increment due to a unit sharp-edge gust
V	velocity, ft/sec
W	weight, lb
w	vertical gust velocity, ft/sec
$\overline{w^2}$	mean square vertical gust velocity, (ft/sec) ²
δ	nondimensional peak acceleration time factor, $\frac{2}{\pi} \omega_n t_p$
ζ	damping ratio, $-a/\omega_n$
σ	root-mean-square acceleration increment, g units

$\hat{\phi}_1(\Omega)$	power-spectral density function of atmospheric turbulence, $\frac{(\text{ft}/\text{sec})^2}{\text{radians}/\text{ft}}$
ω	frequency, radians/sec
ω_n	undamped frequency of airplane short-period oscillation, radians/sec
Ω	frequency, ω/V , radians/ft
Ω_n	frequency, ω_n/V , radians/ft
Ω_o	normalized frequency, Ω/Ω_n
$C_{m\alpha}$	static stability parameter, 1/radians
$C_{L\alpha}$	lift-curve slope, 1/radians
$C_{mq} + C_{m\dot{\alpha}}$	$= \frac{\partial C_m}{\partial \dot{\theta}} \frac{1}{2V} + \frac{\partial C_m}{\partial \dot{\alpha}} \frac{1}{2V}$, damping-in-pitch parameter, 1/radians

MODEL AND INSTRUMENTATION

Model

The principal features of the model are shown in the drawing of figure 1 and the photograph of figure 2. The fuselage had a maximum diameter of 6.5 inches and was constructed of wood with a metal nose section. The wings were 1/4-inch flat plate dural with beveled edges. The important characteristics of the model are listed on figure 1.

Instrumentation

The model was instrumented with a four-channel telemeter which transmitted measurements of normal acceleration, transverse acceleration, total pressure, and fluctuations in total pressure.

Ground instrumentation included a CW Doppler radar for obtaining model velocity, a modified SCR 584 tracking radar for obtaining model position in space and a rawinsonde for obtaining atmospheric conditions. In addition, rollsonde equipment was used for obtaining a measurement of model angular velocity in roll.

The airplane flown in preflight surveys was equipped with a one-channel telemeter which transmitted normal acceleration measurements to the ground receiving station. In addition, the airplane was equipped with standard airspeed acceleration recording instruments.

TEST PROCEDURE

Preflight Turbulence Survey

In reference 1, the atmospheric and turbulence conditions for forecasting and selecting a suitable test day are described in detail. In general, the necessary test condition is clear-air atmospheric turbulence associated with post-cold-front conditions. The test day was chosen on the basis of weather forecasts, and an airplane survey was made over the firing range at the Langley Pilotless Aircraft Research Station, Wallops Island, Va., before the model test as a final check on the suitability of turbulence conditions. The survey also provided a measurement of the variation of turbulence intensity with altitude.

The telemetered normal acceleration measurements from the survey airplane were recorded on a visual recorder while the survey was being made and thus enabled a ground observer to examine for suitability of turbulence conditions. The pilot's judgment of suitable turbulence conditions was used along with the telemetered acceleration data in choosing a suitable test day.

Model Test

Following the airplane survey the model was ground launched at an elevation angle of about 25° by means of a fin-stabilized booster rocket motor. At booster burnout the model separated from the booster and experienced decelerating flight from a Mach number of 0.95 to 0.65. The model flight path was approximately parabolic with a maximum altitude of 1,500 feet. Model free-flight data in continuous turbulence were obtained over a period of about 15 seconds from booster separation to the end of the flight.

ANALYSIS AND RESULTS

Experimental Results

Evaluation of records for Mach number effects.- Acceleration measurements at the model center of gravity were made normal to each wing

of the cruciform configuration. In order to distinguish between the two measurements in this report, one has been called normal and the other transverse acceleration. The telemeter record obtained from the model flight was read at 0.01 second time intervals resulting in a total of 1,540 data points for each accelerometer for the power-off portion of the flight over the Mach number range of 0.917 to 0.66. In order to establish the variation of acceleration increment with Mach number as measured by root-mean-square acceleration, it was necessary to divide the time history of the acceleration measurements into sections and then present the data at the average Mach number for each section. The Mach number and altitude change for each record section along with the average Mach number and altitude and the sample size are shown in table I. From the basic acceleration data for each sample, the acceleration increments from the mean value were computed along with the root-mean-square acceleration increments, σ_{a_n} and σ_{a_t} .

As an illustration of the general characteristics of the acceleration response for the present model, a time history of normal and transverse acceleration increment over the Mach number range of 0.917 to 0.841 is shown in figure 3.

The significant results of the present test are presented in figure 4 as the variation of acceleration increment with Mach number as measured by the root-mean-square acceleration. The results from the two accelerometers σ_{a_n} and σ_{a_t} are shown in figure 4 as measured from the test record and after corrections were made for difference in turbulence intensity at the various altitudes. These corrections were made under the assumption that the horizontal gust velocity obtained from the total-pressure fluctuation data (as described in ref. 2) was representative of the turbulence experienced by each wing. The values of mean square acceleration were corrected for differences in turbulence intensity for the various record sections by multiplying the σ^2 of each record section by the ratio of mean square horizontal gust velocity for the record section near 1,500 feet altitude to the mean square horizontal gust velocity for each record section.

Evaluation of cruciform arrangement.- If the results for each wing shown in figure 4 are considered as having been obtained from two tests of the same model under identical conditions then it should be possible to average the two answers in order to obtain a more accurate answer. This has been done in figure 5 where the variation of σ with Mach number shown was obtained by averaging the $\sigma_{a_n}^2$ and $\sigma_{a_t}^2$ values of figure 4 (corrected to the same turbulence intensity). The spread between the values of σ_{a_n} and σ_{a_t} is also shown on figure 5.

In order to investigate the possibility of testing different wings under identical rough-air conditions by using the cruciform arrangement,

comparisons are made in figure 6 of σ_{an} and σ_{at} for the total record and for cases where the record is divided into progressively smaller sections. The solid line in figure 6 is the line of perfect agreement between the values of σ from the normal and transverse acceleration measurements.

Analytical Calculations

The appendix of this report describes a short and fairly simplified approach for estimating the root-mean-square normal acceleration of aircraft for flight through continuous rough air. The calculated values of σ obtained by using the method and charts of the appendix are compared with the experimental values on figure 5. In order to use the method of the appendix it was necessary to obtain estimates of the following quantities: (a) the spectrum of atmospheric turbulence corresponding to the turbulence intensity at 1,500 feet altitude for the model test, (b) the dynamic stability parameters ω_n and $T_{1/2}$ or ζ , (c) and the model response to a unit sharp-edge gust. As previously mentioned the horizontal gust velocity data were used to correct the experimental data to the turbulence intensity at 1,500 feet altitude; however, these data were not considered adequate for defining the turbulence spectrum. The turbulence spectrum was estimated from the survey airplane data at 1,500 feet altitude, and the following relation, $\phi_1(\omega) = \frac{0.03}{\omega^2}$, was considered reasonable

for making the calculations. Dynamic stability data were not available for the model of this test; however, for the purpose of making calculations for the model of this test, the stability data of reference 3 for a tailless configuration having a similar wing were used. The values of ω_n , $T_{1/2}$ and ζ were obtained by using the data of reference 3 and the weight, inertia, and flight conditions for the model of the present test and are shown in figure 7. The assumed form of the response to a unit sharp-edge gust is shown in figure 8 and is discussed in reference 4 and the appendix of this report.

DISCUSSION

Characteristics of Model Rough-Air Response

The time history of figure 3 indicates that in rough air the short-period frequency is the predominant frequency in the acceleration response. At the Mach numbers of figure 3, the short-period frequency is about 5.50 cycles per second. A high frequency of about 60 cycles per second can also be noted in figure 3. This corresponds to the wing first bending

~~CONFIDENTIAL~~

frequency for the model. By reading the record every 0.01 second it can be seen from figure 3 that the 60-cycle-per-second frequency is not completely included in the data analysis; however, this effect was considered small and the 0.01-second reading interval adequately defines the major frequencies present in the response.

Variation of Acceleration With Mach Number

The variation of root-mean-square acceleration increment with Mach number is presented in figure 4 for accelerations measured normal to each wing. The magnitude of the correction for variations in turbulence intensity is illustrated in figure 4(a) for σ_{a_n} and in figure 4(b) for σ_{a_t} . The correction appears to reduce the scatter and σ_{a_n} and σ_{a_t} show about the same variation with Mach number. There is a fairly rapid increase in σ between Mach numbers 0.816 and 0.88, but this increase is greater for σ_{a_n} . In order to compare measured and calculated root-mean-square accelerations as a function of Mach number, the data of figure 4 have been considered as two separate tests under the same turbulence conditions and were combined as follows on figure 5: $\sigma = \sqrt{\frac{\sigma_{a_n}^2 + \sigma_{a_t}^2}{2}}$.

The experimental data are higher than the calculations; however, the general trend with Mach number is the same for both results. There is a large increase in σ for the calculated curve between Mach numbers 0.92 and 0.95 which is associated with the decrease in damping-in-pitch indicated on figure 7. The large increase in σ for the experimental data occurs at a lower Mach number which may indicate that the damping of the present model deteriorates sooner than was indicated by the calculations. This possibility may exist because the model of the present test had flat plate wings with sharp leading edges while the values of damping-in-pitch derivative $C_{m_q} + C_{m_{\dot{\alpha}}}$ (from ref. 3) used in the calculations were for a configuration having an NACA 0004-65 airfoil.

Evaluation of the Cruciform Arrangement

The results from each wing of the cruciform configuration may be considered to be a separate measurement of the gust loads experience for the configuration. This assumes that there is no mutual interference effects between the two wings and that the atmospheric turbulence input spectrum is the same for each wing. It is not possible to prove these assumptions at this time, but they appear to be reasonable from general considerations of symmetry of the model and of the isotropic nature of the turbulence. The fact that the models usually develop a roll velocity of about 1 radian per second tends to ameliorate any nonisotropic tendencies of the atmospheric turbulence.

Some indication of the accuracy of results from rocket model tests in rough air has been given by considering the present results as separate tests. The spread between the two values of σ is shown on figure 5. The largest differences are about ± 17 percent of the value of σ obtained from combining the two sets of data.

If the two wings are assumed to have about the same turbulence experience, then it should be possible to place different wings on one model in order to investigate such effects as aeroelasticity, and planform. However, the comparison of the results from the two identical wings of the present model indicated large differences of the order of 34 percent, probably due to statistical accuracy as affected by sample size. Due to the short flights and deceleration rate of the model, the sample sizes were limited as shown in table I. Since both wings experienced the same Mach number changes it was possible to make comparisons of σ from each wing for various sample sizes in order to determine what sample size would be necessary to investigate small-order effects of 10 percent or less by means of the cruciform arrangement. These results are shown on figure 6, where the total record has been divided into progressively smaller sections. It appears that a sample size of at least 500 points or 5 seconds of data at nearly constant Mach number would be necessary for testing different wings on the present model. Since the airplane short-period mode of motion is so important in the determination of the mean-square load in rough-air flight, it seems probable that a normalized measure of this time based on the short period frequency and damping characteristics may be found to judge minimum record lengths for other configurations. However, the 5-second sample size should apply to most rocket model tests since all the models have about the same short-period characteristics.

CONCLUDING REMARKS

The present investigation has yielded information on the behavior of a tailless, cruciform 60° triangular-wing configuration in rough-air flight from Mach numbers of 0.66 to 0.88. The variation of root-mean-square acceleration with Mach number indicated a rapid increase between Mach numbers 0.82 and 0.88 that is probably due to a decrease in damping-in-pitch associated with a wing of this plan form.

The use of a cruciform-wing arrangement appears to be useful for improving the accuracy of results from rocket-propelled model tests in rough air under the assumption that the results from each wing may be considered to be a separate measurement of the gust loads experience for the configuration. The extension of the cruciform arrangement for

investigating small-order effects between wings having different characteristics appears to be feasible if a long enough sample at a nearly constant Mach number can be obtained.

Langley Aeronautical Laboratory,
National Advisory Committee for Aeronautics,
Langley Field, Va., December 6, 1955.

~~CONFIDENTIAL~~

APPENDIX

NOTE ON THE CALCULATION OF THE MEAN SQUARE LOADS
OF AIRCRAFT IN CONTINUOUS ROUGH AIR

A basic approach to the problem of the calculation of the mean square loads of aircraft in continuous rough air is given in reference 4. Also, reference 4 gave some examples of mean square load calculations based on a rather simplified assumption as to the form of the airplane response to a sharp edge gust, figure 8. Although it is realized that this picture may be oversimplified, especially for configurations which have high damping, it leads to a fairly simple solution for mean square normal acceleration increments when combined with an atmospheric turbulence spectrum of the form, K_a/Ω^2 . The purpose of the present investigation is to briefly develop and present this solution in the form of a chart which may be used to estimate the mean square normal acceleration increments.

The mean-square normal acceleration is given by the following relation:

$$\sigma^2 = \int_0^{\infty} \hat{\phi}_1(\Omega) |\hat{T}(i\Omega)|^2 d\Omega \quad (1)$$

If the response of the aircraft to a sharp-edge gust is given, as in figure 8, then the amplitude squared of the transfer function which occurs in equation (1) can be expressed as

$$|\hat{T}(i\Omega)|^2 = (a_{n_{\max}})^2 \left\{ \left[\frac{\zeta\Omega_0(1 + \Omega_0^2)\sin \frac{\pi\delta}{2}\Omega_0 + \Omega_0^2(2\zeta^2 - 1 + \Omega_0^2)\cos \frac{\pi\delta}{2}\Omega_0}{(1 - \Omega_0^2)^2 + 4\zeta^2\Omega_0^2} + \frac{\delta^2\Omega_0^2\cos \frac{\pi\delta}{2}\Omega_0}{1 - \delta^2\Omega_0^2} \right]^2 + \left[\frac{\zeta\Omega_0(1 + \Omega_0^2)\cos \frac{\pi\delta}{2}\Omega_0 - \Omega_0^2(2\zeta^2 - 1 + \Omega_0^2)\sin \frac{\pi\delta}{2}\Omega_0}{(1 - \Omega_0^2)^2 + 4\zeta^2\Omega_0^2} + \frac{\delta\Omega_0 - \delta^2\Omega_0^2\sin \frac{\pi\delta}{2}\Omega_0}{1 - \delta^2\Omega_0^2} \right]^2 \right\} \quad (2)$$

Equation (1) comes from equations (29) and (33) of reference 4 while figure 8 and equation (2) represent the general forms of equations (31) and (32) of the same reference.

The power-spectral density function of the atmosphere $\hat{\phi}_1(\Omega)$ for which the present solution was found is the simple expression indicated in references 1, 2, and 6.

$$\hat{\phi}_1(\Omega) = \frac{K_a}{\Omega^2} = \frac{K_a}{\Omega_0^2 \Omega_n^2} \quad (3)$$

It may be noted that for large values of Ω , this is the form of the spectrum which has been given in several places (see ref. 6) as a general form of the spectrum of atmospheric turbulence, that is,

$$\hat{\phi}_1(\Omega) = \frac{\overline{w^2 L}}{\pi} \frac{(1 + 3L^2 \Omega^2)}{(1 + L^2 \Omega^2)^2} \quad (4)$$

or

$$\hat{\phi}_1(\Omega) \rightarrow \frac{\overline{3w^2}}{\pi L} \frac{1}{\Omega^2} \text{ as } \Omega \rightarrow \infty$$

Taking $d\Omega = \Omega_n d\Omega_0$, expanding equation (2) and then substituting, with equation (3), in equation (1), the mean-square normal acceleration can be expressed in the following form which is especially adaptable to presentation in the form of a chart:

$$\left[\frac{\xi \Omega_n}{K_a (a_{n_{\max}})^2} \right] \sigma^2 = \int_0^\infty f(\xi, \Omega_0) d\Omega_0 + \xi \int_0^\infty g(\delta, \Omega_0) d\Omega_0 \quad (5)$$

The first integral, equation (5), containing only ξ and Ω_0 was evaluated in closed form

$$\int_0^\infty f(\xi, \Omega_0) d\Omega_0 = \frac{\pi(1 + \xi^2)}{4} \quad (6)$$

whereas the second integral was approximated by graphical integration (except for the case of δ equal to zero for which the integral was equal to zero by inspection). For practical purposes the integration limits were assumed to be from $\Omega_0 = 0$ to $\Omega_0 = 6$ and the integral

was evaluated for several combinations of ζ and δ to define the mean-square acceleration over a range of ζ and δ .

For the assumption of zero time to peak acceleration, $t_p = 0$ or $\delta = 0$, the mean-square normal acceleration in continuous flight through air having the assumed spectrum is simply that given by the first integral (eqs. (5) and (6))

$$\sigma^2 = \frac{\pi K_a (a_{n_{\max}})^2}{4\Omega_n} \left(\frac{1 + \zeta^2}{\zeta} \right) \quad (7)$$

For any other value of δ , the mean-square normal acceleration is this value plus a part obtained by the numerical integration. Actually for very small values of damping, ζ , equation (7) alone may be used to estimate σ^2 . In this case the mean-square normal acceleration may be further approximated, for $\zeta^2 \ll 1$, after substitution of the appropriate expressions for ζ and Ω_n , as follows:

$$\sigma^2 = 1.133 K_a (a_{n_{\max}})^2 \sqrt{\pi} 1/2 \quad (8)$$

This expression again indicates (see ref. 4) the strong dependence of the mean square loads on the damping characteristics of the oscillatory response to a step gust.

Figure 9 presents the results with the parameter

$$\left[\frac{\zeta \Omega_n}{K_a (a_{n_{\max}})^2} \right] \sigma^2$$

as a function of the damping ratio, ζ , for various values of the non-dimensional peak acceleration time factor, δ . Figure 9 has been computed for values of ζ from 0 to 1.0. Because of the assumptions involved, the chart should be considered most reliable for low values of damping ratio, 0 to 0.25, where the results have been partially checked by rocket-propelled model data.

In order to estimate the mean square acceleration from figure 9, it is necessary to know (1) the initial response of the aircraft to a sharp-edge gust as defined by t_p and $(a_{n_{\max}})^2$ (2) the characteristics of the short period longitudinal oscillation of the aircraft ζ and Ω_n , and (3) the value of the constant K_a of the atmospheric turbulence spectrum. The response to a sharp-edge gust can be obtained from reference 5. The calculation of the characteristics of the short period longitudinal oscillation can be found in many places, but the following approximations are usually satisfactory:

$$\omega_n = \sqrt{\frac{-C_{m_\alpha} q S \bar{c}}{m k_y^2}} \quad (9)$$

$$a = \frac{-qS}{2mV} \left[C_{L_\alpha} - \frac{\left(C_{m_{\dot{\theta} \bar{c}}} + C_{m_{\dot{\alpha} \bar{c}}} \right)}{2 \left(\frac{k_y}{\bar{c}} \right)^2} \right] \quad (10)$$

$$\zeta = \frac{-a}{\omega_n} \quad (11)$$

The evaluation of the turbulence intensity constant, K_a , for a particular application is as yet not very well defined. Some discussion of this factor is given in references 1, 2, and 6.

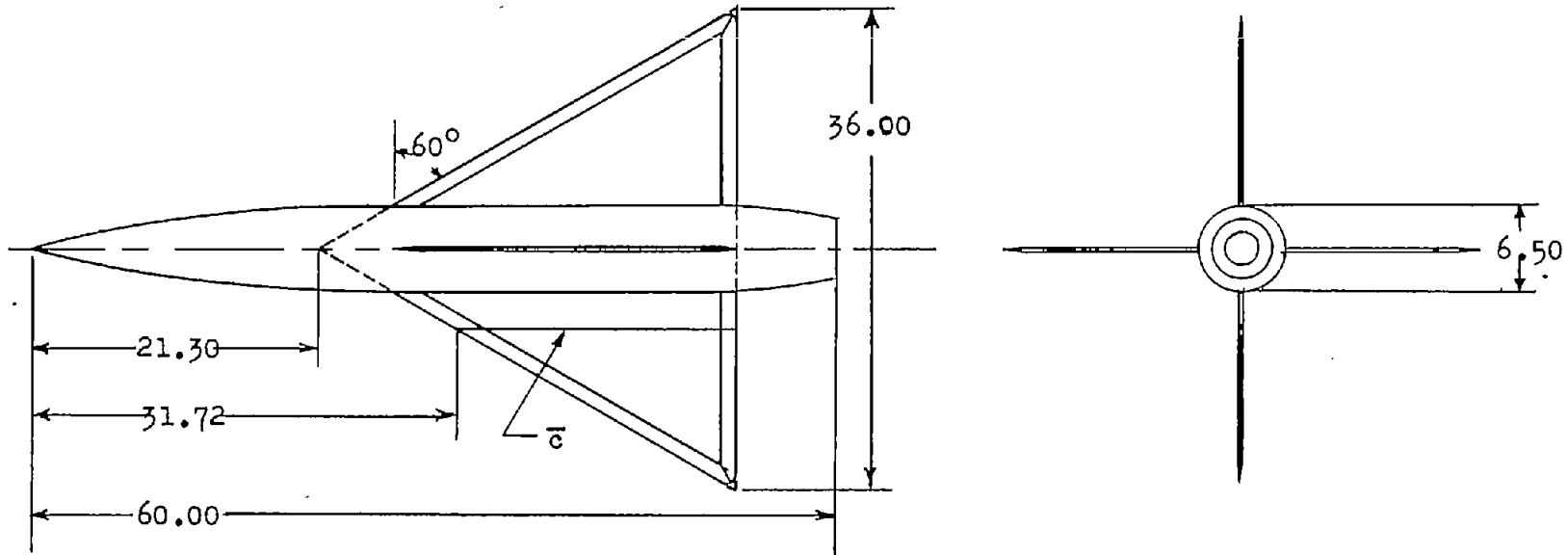
REFERENCES

1. Vitale, A. James, Press, H., and Shufflebarger, C. C.: An Investigation of the Use of Rocket-Powered Models for Gust-Load Studies With an Application to a Tailless Swept-Wing Model at Transonic Speeds. NACA TN 3161, 1954.
2. Vitale, A. James: Characteristics of Loads in Rough Air at Transonic Speeds of Rocket-Powered Models of a Canard and a Conventional-Tail Configuration. NACA RM L54L17, 1955.
3. Beam, Benjamin H., Reed, Verlin D., and Lopez, Armando E.: Wind-Tunnel Measurements at Subsonic Speeds of the Static and Dynamic-Rotary Stability Derivatives of a Triangular-Wing Airplane Model Having a Triangular Vertical Tail. NACA RM A55A28, 1955.
4. Press, Harry, and Mazelsky, Bernard: A Study of the Application of Power-Spectral Methods of Generalized Harmonic Analysis to Gust Loads on Airplanes. NACA Rep. 1172, 1954. (Supersedes NACA TN 2853.)
5. Mazelsky, Bernard: Charts of Airplane Acceleration Ratio for Gusts of Arbitrary Shape. NACA TN 2036, 1950.
6. Press, Harry, and Meadows, May T.: A Reevaluation of Gust-Load Statistics for Applications in Spectral Calculations. NACA TN 3540, 1955.

TABLE I

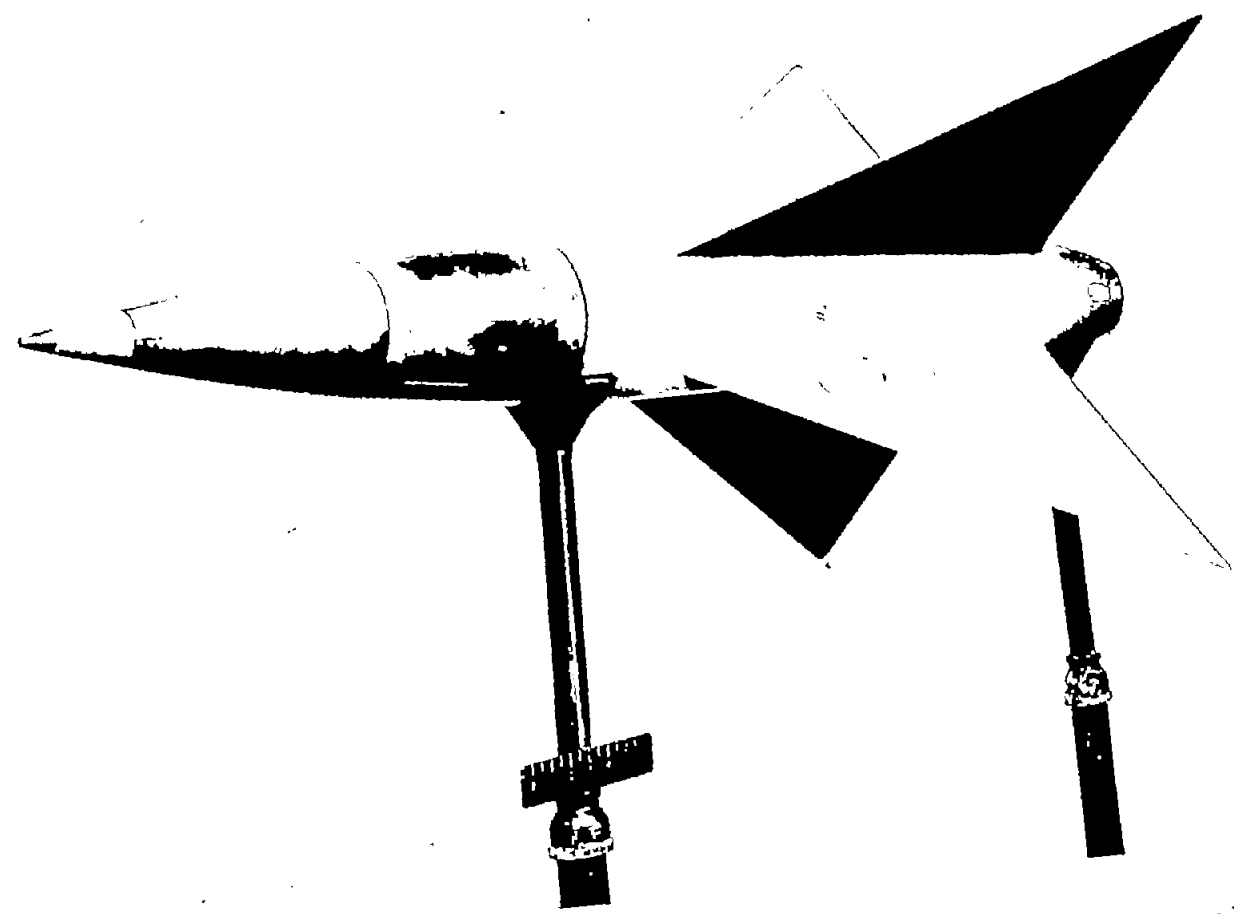
VARIATION OF MACH NUMBER AND ALTITUDE

Mach number of sample	Sample size, number of points	Altitude, ft
0.878 ± 0.0433	200	860 ± 210
$.816 \pm .0300$	200	$1,260 \pm 190$
$.766 \pm .0340$	300	$1,425 \pm 25$
$.718 \pm .0307$	400	$1,185 \pm 215$
$.678 \pm .0265$	440	485 ± 485



S, ft ²	3.90
W, lb	93
I _y , I _z , slug-ft ²	2.88
\bar{c} , ft	1.73
c.g. position, percent \bar{c}	24

Figure 1.- Drawing of model. All dimensions are in inches.



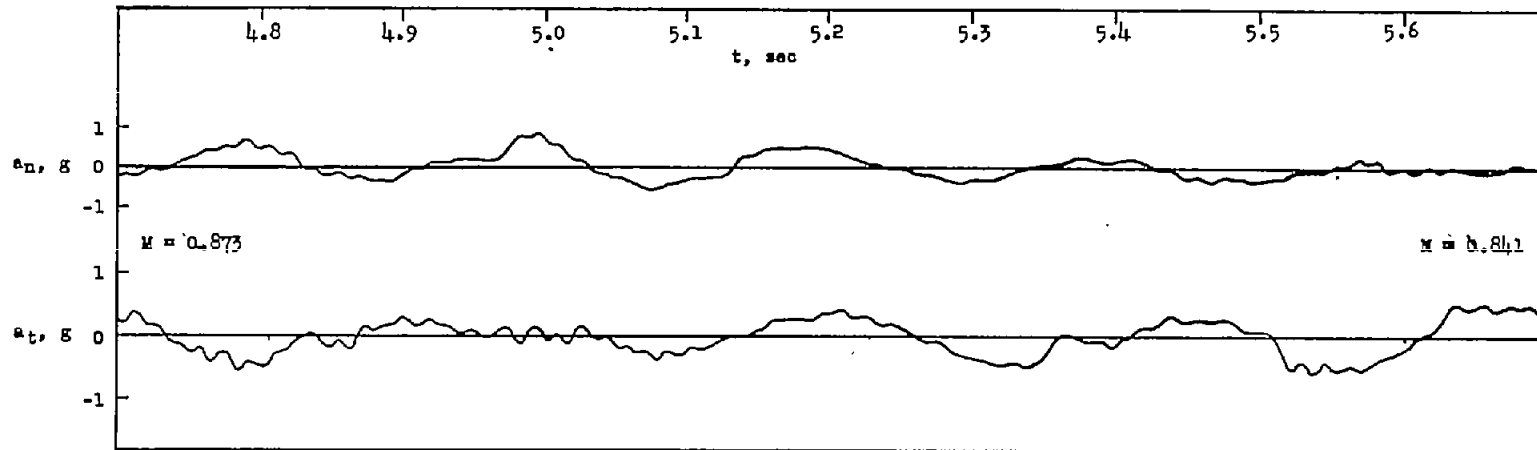
CONFIDENTIAL

CONFIDENTIAL

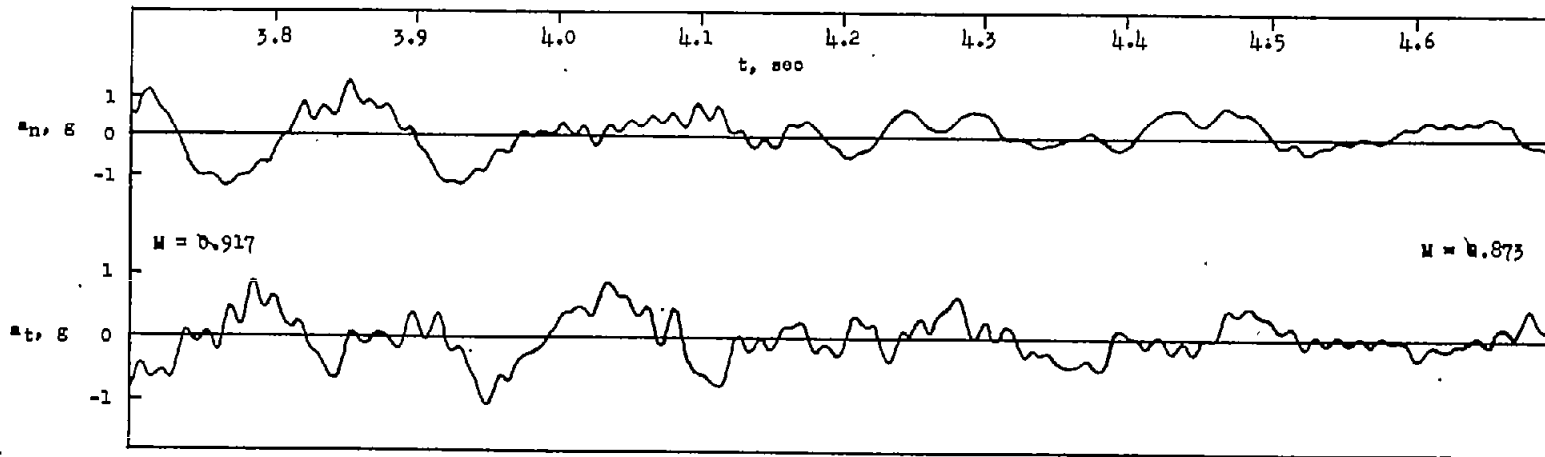
NACA RM 155128

L-82428.1

Figure 2.- Photograph of model.

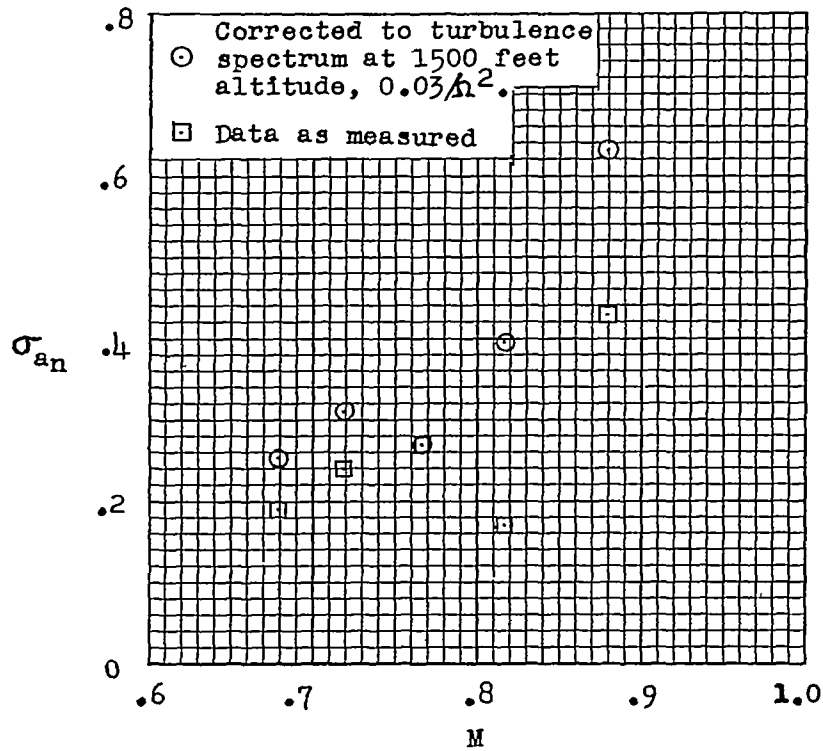


(a) Mach number changing from 0.841 to 0.873.

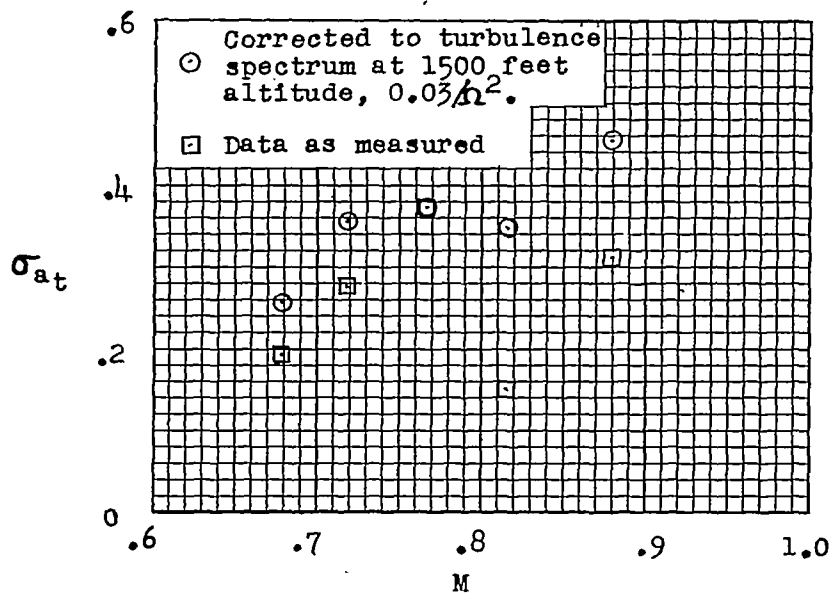


(b) Mach number changing from 0.873 to 0.917.

Figure 3.- Typical time histories of normal and transverse acceleration.



(a) Normal acceleration.



(b) Transverse acceleration.

Figure 4.- Variation of root-mean-square acceleration with Mach number.

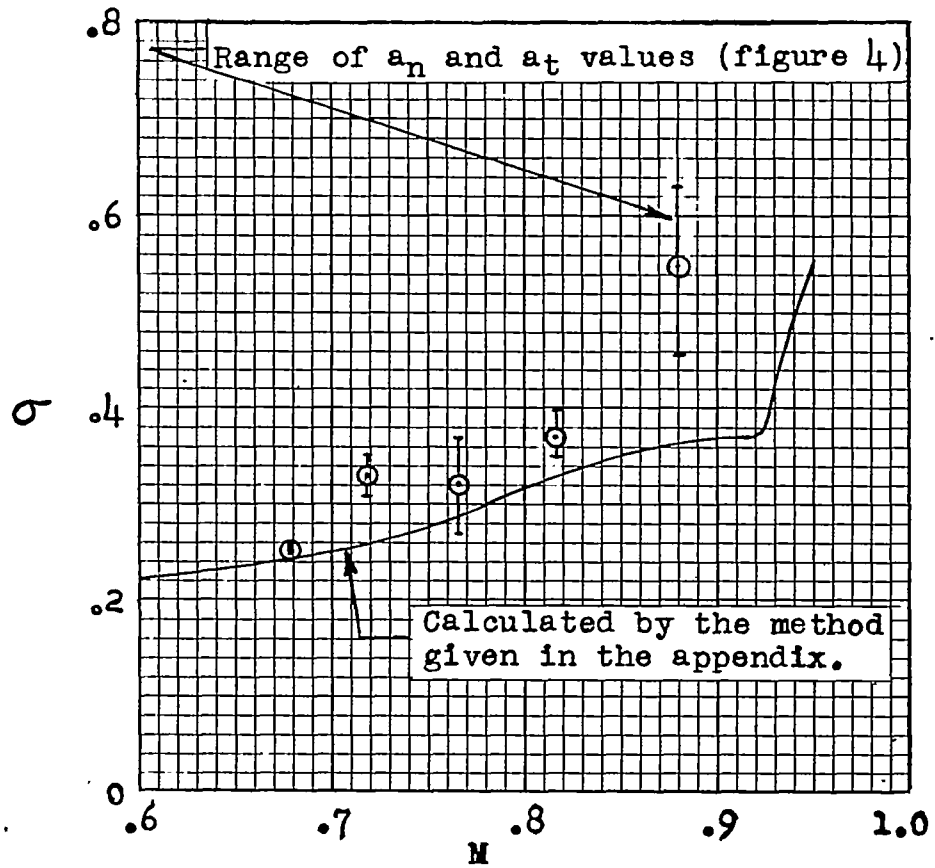


Figure 5.- Variation with Mach number of root-mean-square acceleration obtained by combining a_n and a_t .

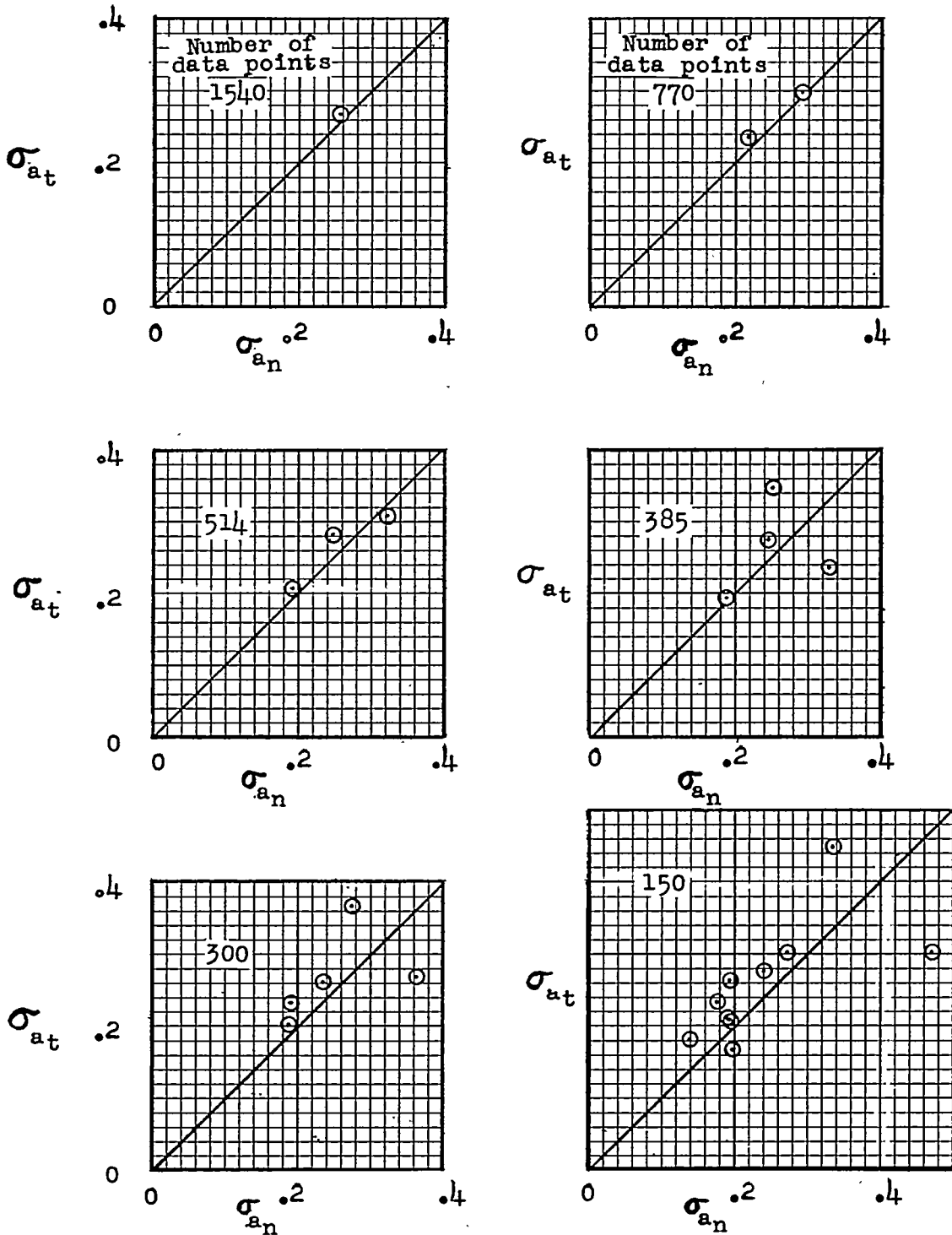
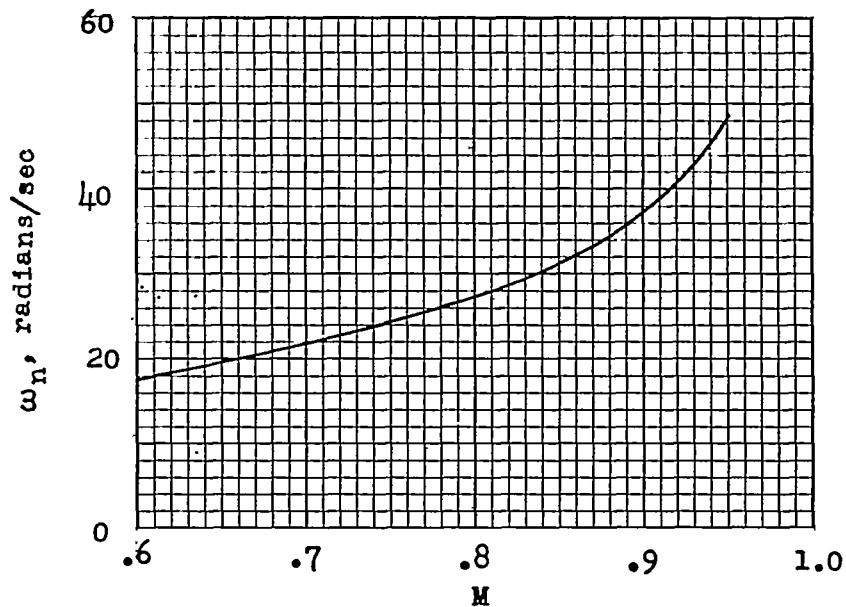
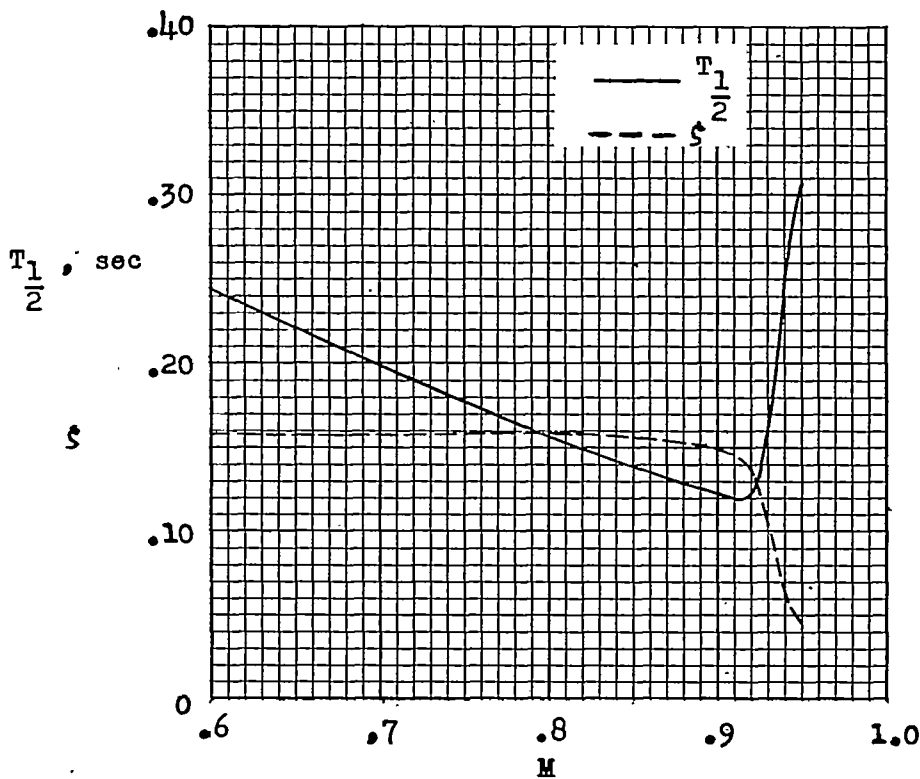


Figure 6.- Comparison of root-mean-square acceleration obtained from normal and transverse accelerometers for several sample sizes.



(a) Variation of undamped natural frequency with Mach number.



(b) Variation of $T_1/2$ and ζ with Mach number.

Figure 7.- Stability characteristics of model.

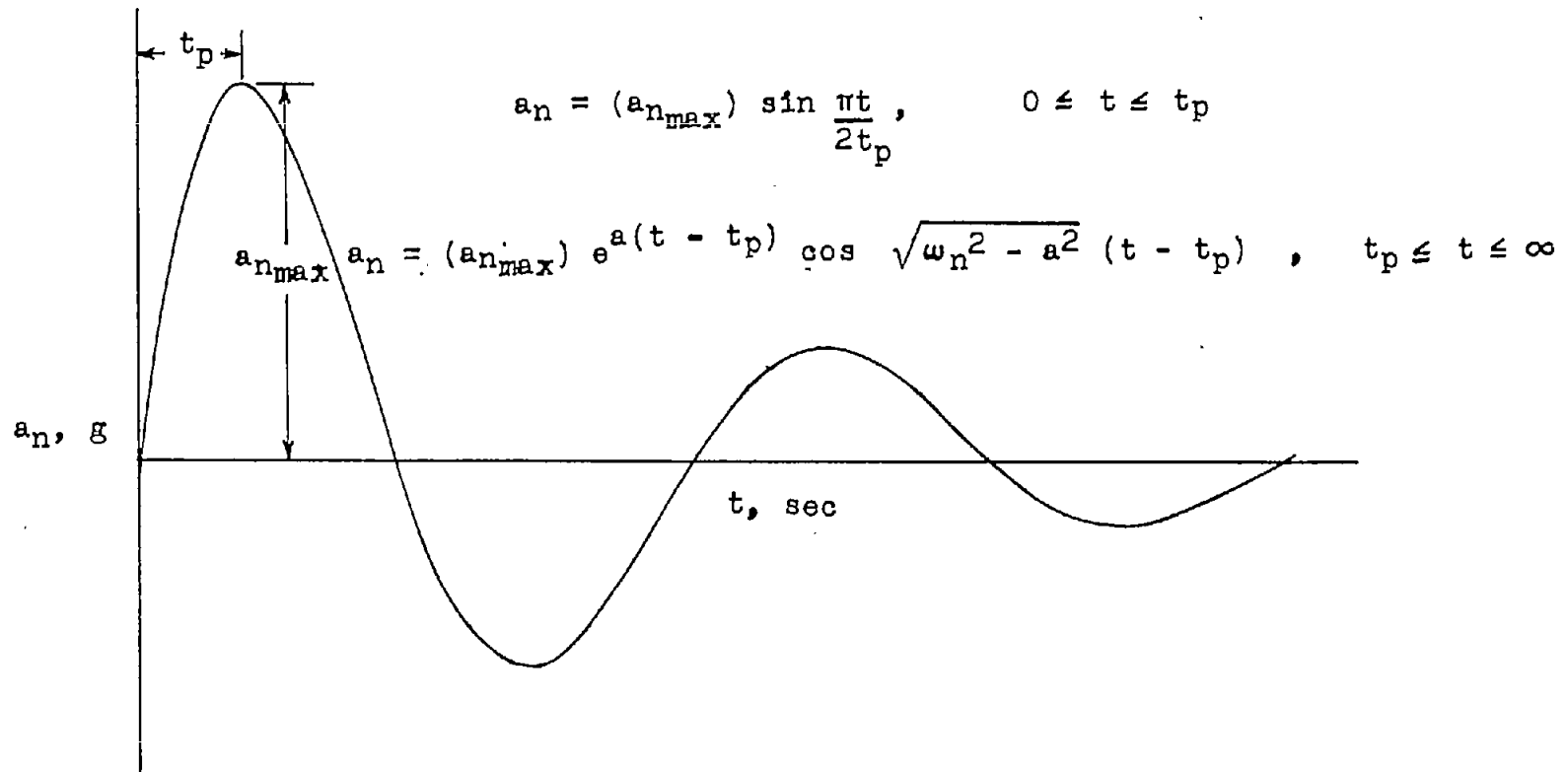


Figure 8.- The assumed response to a unit sharp-edge gust.

~~CONFIDENTIAL~~

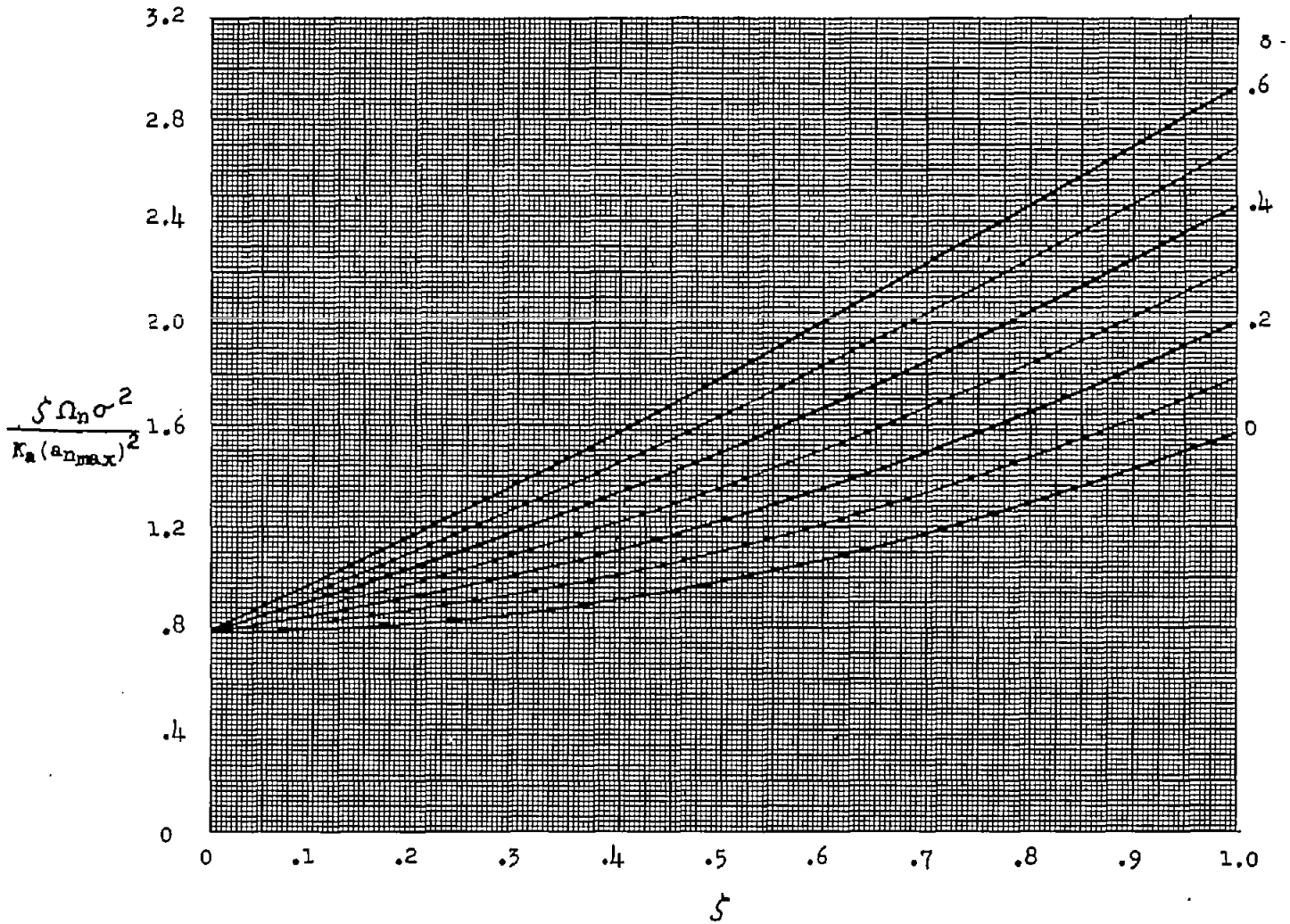


Figure 9.- Chart for the determination of the mean-square normal acceleration response of aircraft in continuous rough air.

~~CONFIDENTIAL~~
 156
 156

~~CONFIDENTIAL~~